

Plasticity over a wide range of strain rates and temperatures

S. R. BODNER

*Faculty of Mechanical Engineering
Technion – Israel Institute of Technology
Haifa 32000, Israel.*

A NUMBER of constitutive theories of elastic-viscoplastic deformation were proposed over the past years which have been found useful for practical applications. Most of them use the second invariant of deviatoric stress, as identified by Huber, as the effective stress driving inelastic deformations. This paper examines a particular constitutive theory, that of Bodner–Partom, over a very wide range of strain rates and temperatures.

1. Introduction

MACROSCOPIC CONSTITUTIVE EQUATIONS for elastic-viscoplastic material behavior should be consistent with the overall physics of inelastic deformation and in accord with the principles of mechanics and thermodynamics. Basic for the formulation would be a kinetic equation relating the inelastic strain rate to the stress, temperature and internal state variables such as those representing resistance to inelastic deformation – the hardening variables. Those variables are load history dependent and are determined from auxiliary evolution equations. Constitutive theories of this class are considered to be “unified” for which creep and stress relaxation are response characteristics obtained from the same set of equations for different loading conditions. Some of these theories are reviewed in the books edited by MILLER [1] and by LEMAITRE [2]. Constitutive theories that do not rely on a yield criterion to isolate a fully elastic region could be considered to be “unified” in a more general sense.

For metals, the most relevant physical mechanism for inelastic straining is thermally activated dislocation generation and motion on slip planes. The present paper examines the constitutive theory of Bodner–Partom (B–P) [3, 4], which is of thermal activation form, for extreme cases of temperature and strain rate to check its consistency with physical reality. Temperatures are considered over the full range from absolute zero to melting and strain rates over 14 decades from 10^{-8} s^{-1} to 10^6 s^{-1} . Also, some comments are made on the matter of incorporating possible size effects into the theory. A summary of the B–P equations for

small strains and isotropic behavior is provided here with explanations of the various material constants.

2. Outline of the B-P elastic-viscoplastic theory

The kinetic equation for inelastic strain rate of the B-P formulation is given by

$$(2.1) \quad \dot{\epsilon}_{ij}^P = D_0 \exp \left[-\frac{1}{2} \left(\frac{Z^2}{\sigma_{\text{eff}}^2} \right)^n \right] \frac{\sqrt{3} s_{ij}}{\sigma_{\text{eff}}}; \quad \dot{\epsilon}_{kk}^P = 0$$

with

$$\sigma_{\text{eff}} = (3J_2)^{1/2} = \left(\frac{3}{2} s_{ij} s_{ij} \right)^{1/2},$$

which was motivated by correspondence of the form and parameters with general response characteristics. It is consistent with the Prandtl-Reuse flow law and indicates incompressibility of inelastic deformations. Also, it is a typical growth curve that has been used in diverse fields with sections of incubation, rapid growth, and the tendency to saturation. For the case of uniaxial stress σ_{11} , Eq. (2.1) reduces to

$$(2.2) \quad \dot{\epsilon}_{11}^P = \frac{2}{\sqrt{3}} \left(\frac{\sigma_{11}}{|\sigma_{11}|} \right) D_0 \exp \left[-\frac{1}{2} \left(\frac{Z}{\sigma_{11}} \right)^{2n} \right]$$

which is represented in Fig. 1 and is practically limited to $(\sigma_{11}/Z) < 1$.

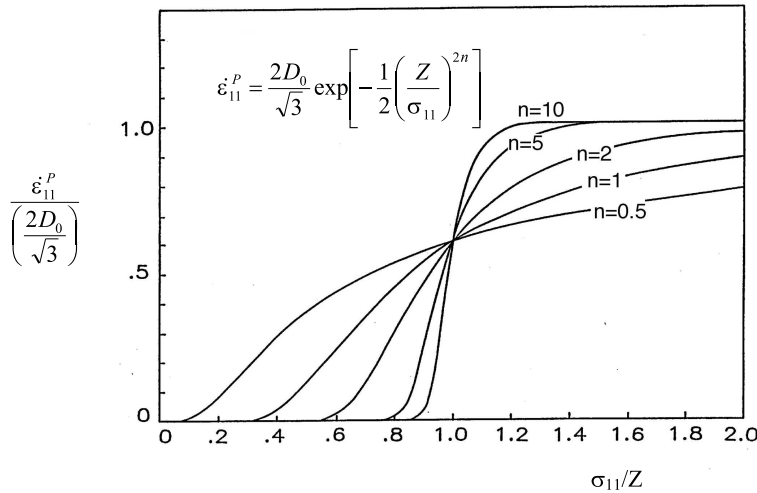


FIG. 1. Inelastic strain rates for uniaxial tension, σ_{11} and various values of n .

Noted in Fig. 1 is the flat incubation period at low stresses with low levels of plastic straining which is required for a plasticity theory without a discrete yield criterion. In such a theory, the total strain rate is considered to consist of elastic and inelastic components, $\dot{\epsilon}_{11} = \dot{\epsilon}_{11}^e + \dot{\epsilon}_{11}^p$ which are generally non-zero. The coefficient D_0 in Eq. (2.1) would be the limiting strain rate in shear for large stress. It is seen in Fig. 1 that the parameter n controls rate sensitivity and as n becomes large for a given plastic strain rate, the non-dimensional term σ_{11}/Z approaches unity and its rate dependence diminishes. Rate independent plasticity is therefore a limiting case in the formulation.

The hardening parameter Z in Eq. (2.1) represents resistance to inelastic deformation and is assumed to consist of an isotropic component, Z^I , and a scalar effective value Z^D , which is the component of the directional hardening tensor, β_{ij} , in the direction of the current stress, u_{ij} . These quantities are load history dependent and are obtained by associated evolution equations,

$$(2.3) \quad \dot{Z}^I(t) = m_1[Z_1 - Z^I(t)]\dot{W}_p(t) - A_1 Z_1 \left[\frac{Z^I(t) - Z_2}{Z_1} \right]^{r_1} : Z^I(0) = Z_0,$$

$$(2.4) \quad \dot{\beta}_{ij}(t) = m_2 [Z_3 u_{ij}(t) - \beta_{ij}(t)] \dot{W}_p(t) - A_2 Z_1 \left\{ \frac{[\beta_{kl}(t)\beta_{kl}(t)]^{1/2}}{Z_1} \right\}^{r_2} v_{ij}(t) : \beta_{ij}(0) = 0$$

with

$$(2.5) \quad Z^D = \beta_{ij} u_{ij},$$

where

$$(2.6) \quad u_{ij}(t) = \sigma_{ij}(t)/[\sigma_{kl}(t)\sigma_{kl}(t)]^{1/2}$$

and

$$(2.7) \quad v_{ij}(t) = \beta_{ij}(t)/[\beta_{kl}(t)\beta_{kl}(t)]^{1/2},$$

where v_{ij} is the current direction of β_{ij} .

For the evolution equation for isotropic hardening Z^I , Eq. (2.3), the second term indicates static recovery, generally due to low strain rates at relatively high temperature, with Z_2 as the stable (minimum) value at a given temperature, and A_1 and r_1 are material constants. In the absence of recovery, Z_1 would be the saturation value of Z and \dot{W}_p represents the plastic work rate which is considered to be the generator of hardening. Plastic work, rather than effective plastic strain,

is taken to be the measure of hardening to obtain agreement with strain rate jump tests. The evolution equation for directional hardening, represented by Eq. (2.4), has the same general form as that for isotropic hardening. By the definition of Z^D , Eq. (2.5), reversal of stress would lead to reduction of hardening referred to as the Bauschinger effect. The rate of directional hardening, m_2 , is usually appreciably larger than that for isotropic hardening, m_1 , which is useful in parameter identification.

Methods for determining the material constants and the results of applications of the B-P theory are described in [4]). Some of the parameters are temperature-dependent over the range of applicability. Of interest is the examination of the theory for the extreme conditions of temperature and strain rate and the matter of possible size effects.

3. Limiting conditions

As noted, the B-P constitutive equations are intended to be a macroscopic representation of inelastic deformation due to thermally activated dislocation motion. The coefficient D_0 in Eqs. (2.1) and (2.2) corresponds to the limiting (maximum) strain rate for large stress. It is essentially a scale factor and should be initially specified in procedures for obtaining the material parameters from test results [4, 5]. A limitation on the choice of D_0 is that the strain rates in the applications should be at least two decades less than D_0 .

From the physical viewpoint, D_0 would be the maximum strain rate possible for thermally activated dislocation slip to take place. Based on the simplified Orowan equation for plastic slip and the maximum values of mobile dislocation density and velocity for metals indicated in the literature, the approximate value for the maximum distortional strain rate is of order 10^8 s^{-1} with material dependent variations. This value was used for D_0 in recent exercises that involved strain rates as high as 10^6 s^{-1} . A lower value for D_0 , 10^4 s^{-1} , was used in earlier work that involved low strain rates to avoid possible numerical difficulties.

It has been observed that some metals, notably pure copper and aluminum, exhibit increased strain rate sensitivity for strain rates above about 10^4 s^{-1} . This appears to be due to a large increase in the hardening rate, but the physical mechanism is unclear at this stage. A reasonable procedure for modifying the equations would be to take the hardening rate to be itself a function of strain rate with the saturation hardening values remaining unchanged. That would be necessary for the effect to be non-reversible for changes in strain rates. This modification would mean that the stress-strain relation would approach the saturated stress value at an increased rate. Comparison of this procedure, described in [6], with test results from [7] are shown in Fig. 2.

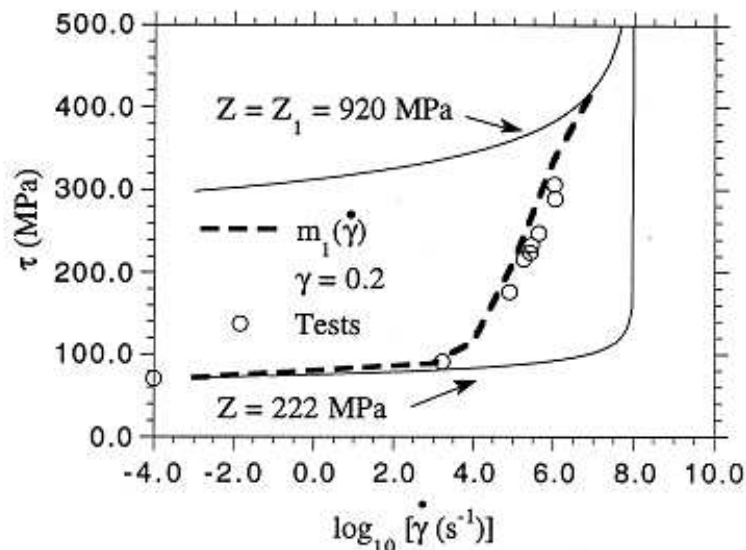


FIG 2. Flow stress dependence of copper on logarithm of the strain rate, a) original B-P model for $Z = 222$ MPa (corresponding to $\gamma = 0.20$ at the lower rates), and for the stress saturation condition with $Z = Z_1 = 920$ MPa: ——— b) modified B-P model with strain rate dependence of the hardening rate, from BODNER and RUBIN [6]: - - - - - experimental points for $\gamma = 0.20$, TONG *et al.* [7]: ○○○.

Despite the interpretation of D_0 , there should be no physical limit to the distortional strain rate to which a material could be subjected. Inversely, it means that the thermally activated dislocation slip mechanism is inoperative at very high strain rates due to the breakdown of the crystalline lattice. This was shown in molecular dynamics simulations of atomic arrays with dislocation type defects [8]. These simulations suggest that the response of a crystalline solid transits to viscous fluid-like behavior at melting and at very high strain rates. A more recent investigation [9] on inelastic deformation of metals indicates that work hardening could be neglected at very high strain rates where overdriven shocks become operative. In exercises for copper and tantalum, the transition from crystalline slip to shock conditions with viscous fluid-like response behavior occurs at a strain rate of about 10^8 s $^{-1}$, Figs. 11, 12 of [9].

There is also no lower limit on time-dependent inelastic straining as is known from the very slow creep of geological materials. For metals under constant uniaxial stress, Eqs. (2.2), (2.3) apply. At relatively high strain rates, the recovery term in Eq. (2.3) would be unimportant and hardening would saturate at $Z^I = Z_1$ with the stress reaching its maximum steady value. Under the influence of recovery at intermediate strain rates, a condition could be reached where the

rate of recovery equals the rate of hardening. This leads to $\dot{Z}^I \rightarrow 0$ and steady state (secondary) creep ensues since σ_{11} and Z^I are constant. The value of Z at this steady condition would be less than Z_1 . At relatively low strain rates, the recovery term would dominate. Plots of the log of steady strain rates against the associated applied stress levels therefore indicate three distinct branches, each having a different slope, e.g. Fig. 7 of [4]. Calculated results for two metals at high temperature based on Eqs. (2.2), (2.3) compare well with available test data in the range 10^{-8} s^{-1} to 10^{-3} s^{-1} , Fig. 7 of [4]. The material constants used in the exercise were obtained from controlled tensile straining tests.

With regard to the capability of the B-P theory to represent thermal effects, determination of the material parameters from constant temperature tests proved to be adequate for varying thermal conditions. That is, temperature history effects appear to be unimportant for most materials except for those that experience dynamic strain aging. For the B-P equations, some of the individual parameters are temperature dependent and an overall single representation of temperature in the kinetic equation does not seem adequate. The parameters mostly influenced by temperature are n , $Z_0 = Z_2$, Z_1 , Z_3 and the recovery coefficients A_1 , A_2 .

It is seen in Fig. 1 that the material constant n controls rate sensitivity and also influence the level of the stress-strain relation. Test results indicate that n generally varies inversely with T so strain rate sensitivity increases with increasing T and the material experiences lower stress levels. The parameter n could also be a function of pressure p , but that is not considered here. To demonstrate thermal effects analytically, simplistic expressions of $n(T)$ and $Z(W_p, T)$ are assumed:

$$(3.1) \quad Z(W_p, T) = R(T) Z(W_p),$$

$$(3.2) \quad n(T) = (C/T) \{1 - [(T - T_0)/(T_m - T_0)]^q\}, \quad T > T_0$$

$$(3.3) \quad R(T) = 1 - [(T - T_0)/(T_m - T_0)]^s, \quad T > T_0$$

where T is the current temperature, T_m is melting, T_0 is a reference temperature, and C, q, s are material constants. For $T = 0^\circ \text{ K}$, n becomes infinite and $R = 1$ leading to strain rate independent behavior, and $\sigma_{11} = Z(W_p)$, Fig. 1, so that Z is referred to as the ‘‘mechanical threshold stress’’. As expected, thermally activated dislocation motion ceases at 0° K .

At temperatures intermediate from 0° K to T_m , the strain rate sensitivity parameter n and some, or all, of the hardening parameters, Z_0 , Z_1 , Z_2 and Z_3 and the recovery parameters A_1 , A_2 , r_1 and r_2 , can be functions of temperature.

Lists of these dependences for a number of metals are given in [4]. Because of the availability of test results for Copper at various temperatures at a single high strain rate, $2000s^{-1}$, an exercise was performed [10] to see if taking Z_1 to be a function of T could match the data. Test results at different strain rates were not available so that n was a fixed value in the simulations and $R(T)$ was taken to be bilinear. The matching was fairly good, Fig. 3, but tests at various strain rates would be required for more complete identification of the material parameters.

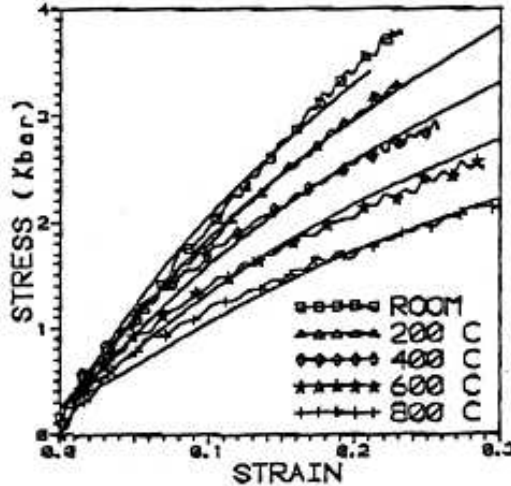


FIG. 3. Comparison of the experimental data of GRAY *et al.* for compression of copper at a strain rate $2000s^{-1}$ with the Bodner–Partom model simulations taking $Z_1 \rightarrow Z_1(T)$, from BODNER and RAJENDRAN [10].

As T approaches T_m , and R from Eqs. (3.2), (3.3) tend to zero so that $\dot{\epsilon}_{11}^P$ nears its limiting value,

$$(3.4) \quad \dot{\epsilon}_{11}^P = (2/\sqrt{3})D_0.$$

The thermally activated inelastic straining mechanism is therefore inoperative as $T \rightarrow T_m$ and the material response would be that of a nonlinear viscous fluid whose characteristics would be governed, in part, by the physics of melting. As discussed previously, this behavior is similar to that at very high strain rates but the governing relationships would be different.

On the matter of size effects, these are not indicated in the B–P theory which applies to material in bulk. Recent tests on samples of micrometer sized dimensions, UCHIC *et al.* [11] show a definite increase in stress level from that of the bulk material, Figs. 1, 2 of [11]. The authors of [11] surmise that the small sample dimensions limit the length scales available for plastic flow processes. In terms

of the B–P equations, this effect can be interpreted as an increase in the value of the hardening saturation value Z_1 , with decrease in sample size to micrometer-sized dimensions. Another interpretation is that the small specimen size limits the mobile dislocation density with the result that D_0 would be reduced from its value for the bulk condition. Reduction of D_0 with the other material constants obtained for the bulk condition remaining the same would lower $\dot{\epsilon}_{11}^P$ and increase the stress level. The B–P equations can therefore accommodate the size effect in a direct but empirical manner.

Further tests such as reported in [11] performed at various strain rates and temperatures would be highly desirable for the purpose.

References

1. A. K. MILLER [Ed.], *Unified constitutive equations for creep and plasticity*, Elsevier Applied Science Pub., London 1987.
2. J. LEMAITRE [Ed.], *Handbook of materials behavior models*, Academic Press, San Diego, CA, 2001.
3. S. R. BODNER and Y. PARTOM, *Constitutive equations for elastic-viscoplastic strain-hardening materials*, ASME J. Appl. Mech., **42**, 385–398, 1975.
4. S. R. BODNER, *Unified plasticity for engineering applications*, Kluwer Academic/Plenum Pub., New York 2002.
5. R. MAHNKEN and E. STEIN, *Parameter identification for viscoplastic models based on analytical derivatives of a least-squares functional and stability investigations*, Int. J. Plasticity, **12**, 4, 451–479, 1996.
6. S. R. BODNER and M. B. RUBIN, *Modeling of hardening at very high strain rates*, J. Appl. Phys., **76**, 5, 2742–2747, 1994.
7. W. TONG, R. J. CLIFTON and S. HUANG, *Pressure-shear impact investigation of strain rate history effects in oxygen – free high-conductivity copper*, J. Mech. Phys. Solids, **40**, 1251–1294, 1992.
8. B.L. HOLIAN and P.S. LOMDAHL, *Plasticity induced by shock waves in nonequilibrium molecular-dynamics simulations*, Science, **280**, 2085–2088, 1998.
9. D.L. PRESTON D.L. TONKS and D.C. WALLACE, *Model of plastic deformation for extreme loading conditions*, J. Applied. Physics, **93**, 1, 211–220, 2003.
10. S.R. BODNER and A.M. RAJENDRAN, *On the strain rate and temperature dependence of hardening of copper*, Proc. of the Conf. of the Amer. Physical Society, Topical Group on Shock Compression of Condensed Matter, Seattle, Washington (1995), AIP Press, 499–502, 1996.
11. M. D. UCHIC, D. M. DIMIDUK, J. N. FLORANDO, W. D. NIX, *Sample dimensions influence strength and crystal plasticity*, Science, **305**, 986–989, 2004.

Received October 22, 2004.
